

**Development of polymer microcapsules functionalized with fucoidan to target P-selectin  
overexpressed in cardiovascular diseases**

*Bo Li, Maya Juenet<sup>#</sup>, Rachida Aid-Launais<sup>#</sup>, Murielle Maire, Véronique Ollivier, Didier  
Letourneur and Cédric Chauvierre<sup>\*</sup>*

Bo Li, Maya Juenet, Rachida Aid-Launais, Murielle Maire, Véronique Ollivier, Didier Letourneur,  
Cédric Chauvierre

INSERM, U1148, Laboratory for Vascular Translational Science; CHU X. Bichat, Paris Diderot  
University; 46 rue H. Huchard, 75018 Paris, & Institut Galilée, Paris 13 University; 99 av JB Clément,  
93430 Villetaneuse, France

<sup>\*</sup> E-mail: cedric.chauvierre@inserm.fr

<sup>#</sup> Equivalent work

Keywords: polymer microcapsules, fucoidan, P-selectin, thrombosis, molecular targeting

## ABSTRACT

New tools for molecular imaging and targeted therapy for cardiovascular diseases are still required. Herein, biodegradable microcapsules (MCs) made of polycyanoacrylate and polysaccharide and functionalized with fucoidan (Fuco-MCs) were designed as new carriers to target arterial thrombi overexpressing P-selectin. Physico-chemical characterizations demonstrated that microcapsules have a core-shell structure and that fucoidan was present onto the surface of Fuco-MCs. Furthermore, their size ranged from 2 to 6  $\mu\text{m}$  and they were stable on storage over 30 days at 4°C. Flow cytometry experiments evidenced the binding of Fuco-MCs for human activated platelets as compared to MCs (MFI: 12,008 vs 9,  $P < 0.001$ ) and its absence for non-activated platelets (432). An *in vitro* flow adhesion assay showed high specific binding efficiency of Fuco-MCs to P-selectin and to activated platelet aggregates under arterial shear stress conditions. Moreover, both types of microcapsules revealed excellent compatibility with 3T3 cells in cytotoxicity assay. One hour after intravenous injection of microcapsules, histological analysis revealed that Fuco-MCs were localized in the rat Abdominal Aortic Aneurysm thrombotic wall and that the binding in the healthy aorta was low. In conclusion, these microcapsules appear as promising carriers for targeting of tissues characterized by P-selectin overexpression and for their molecular imaging or treatment.

## 1. Introduction

P-selectin, an adhesion molecule, is expressed at the surface of activated platelets and injured vascular endothelium. Therefore, P-selectin is a marker of biologically active arterial thrombi and expansion of Abdominal Aortic Aneurysms (AAA).<sup>[1]</sup> In recent studies, P-selectin was described as a molecular imaging target for AAA early detection, dilatation and rupture risk assessment. Some authors have developed nano/micro-contrast agents for imaging of P-selectin using ultrasound or magnetic resonance.<sup>[2]</sup> Limitations are related to the low binding efficiency in high blood shear rate of nano/microspheres to P-selectin on the area of AAA leading to not sufficient detectable contrast signals for predicting AAA rupture risk. Moreover, microspheres as compared to nanospheres showed higher margination efficiency in recirculating blood flow and thus may be an advantage for treatment of arterial thrombi.<sup>[3]</sup> New carrier systems with strong P-selectin binding are still needed for vascular-targeted imaging or drug delivery.

Fucoidan, a seaweed-derived polysaccharide with sulfated chains, was proved to be an efficient glycosidic ligand of P-selectin.<sup>[4]</sup> Our group previously demonstrated its ability to bind P-selectin and developed a radiotracer by combining Technetium (<sup>99m</sup>Tc) to fucoidan to enable detection of activated endothelium and thrombosis.<sup>[5]</sup> Recently, we developed fucoidan functionalized iron oxide nanoparticles and polysaccharide microparticle radiolabeled with <sup>99m</sup>Tc, for MRI or SPECT imaging respectively.<sup>[6]</sup>

The aim of the present study was to produce by an easy way injectable polymer microcapsules able to target P-selectin. The first design of biodegradable poly(alkylcyanoacrylate) (PACA) nanoparticles prepared by emulsion polymerization as *in vivo* drug delivery carrier was described in 1979.<sup>[7]</sup> The classical approach for the preparation of PACA nanoparticles is the emulsion polymerization by either anionic or redox radical mechanisms.<sup>[8-10]</sup> Different types of PACA nanosystems have been

developed in the past decades such as polymer nanoparticles,<sup>[11]</sup> core-shell polymer nanoparticles<sup>[12]</sup> and polymer nanocapsules.<sup>[13]</sup> Moreover, a great variety of bioactive compounds have been loaded on these different types of PACA nanosystems<sup>[14]</sup> such as antioxidant agents,<sup>[15]</sup> anticancer drugs,<sup>[16]</sup> antibiotics,<sup>[17]</sup> proteins,<sup>[18]</sup> peptides<sup>[19]</sup> and nucleic acids.<sup>[13, 20]</sup> However, issues still exist such as the initiation of the polymerization reaction of alkylcyanoacrylates by the chosen reactive drug instead of by the hydroxyl ions for anionic mechanism or by free radicals for redox radical mechanism. To overcome these limitations, Yordanov G. *et al* recently reported the preparation of poly (butylcyanoacrylate) (PBCA) homopolymer nanospheres by the nanoprecipitation method using a pre-synthesized polymer and colloidal stabilizers.<sup>[21]</sup> Nevertheless, this method requires multiple steps for obtaining PACA nanospheres. We report here a new process to obtain microcapsules that are assembled from polymerization of isobutyl cyanoacrylate (IBCA) in presence of perfluorooctyl bromide (PFOB), coated by polysaccharides and functionalized with fucoidan. The choice of perfluorooctylbromide was based on two main reasons. Firstly, perfluorooctylbromide can be used as a contrast agent for ultrasonography and <sup>19</sup>F Magnetic Resonance Imaging (MRI). Perfluorooctylbromide microcapsules functionalized with fucoidan could therefore be used as contrast agents for the molecular imaging of cardiovascular diseases Secondly it was used here as a model carrier for loading active agents with regard to its hydrophobic property, some hydrophobic drugs (e.g. curcumin) could be considered to be loaded into the hydrophobic core of the microcapsules by following the same synthesis method. The thickness of the microcapsules can be adjusted by simply modifying the pH value of the water phase prior to emulsification. Flow cytometry and flow chamber experiments were performed to evaluate the specificity of the interaction between activated platelets and microcapsules functionalized with fucoidan (Fuco-MCs). In addition, *in vivo* experiments performed in an elastase-induced AAA rat model showed that

Fuco-MCs were located in the thrombotic abdominal aorta and not in healthy rats which confirms the ability of these microcapsules to target specifically P-selectin. These microcapsules appear as new tools to image at molecular level or to treat cardiovascular pathologies in which P-selectin is overexpressed.

## 2. Results

### 2.1. Preparation and characterization of microcapsules

New polymer microcapsules coated with polysaccharides and loaded with PFOB were prepared by modification of the commonly used emulsion-evaporation polymerization process (**Figure 1**). According to previous studies,<sup>[4, 9, 22, 23]</sup> PACA nanoparticles are synthesized at low pH values to avoid anionic homopolymerization occurring spontaneously due to the rapid initiation by the hydroxyl groups of water. However, it was impossible to form microcapsules at a pH value lower than 3 (**Table 1**). In contrast, when the pH value was either set to 7 or 10 at 30°C, the microcapsule mass yield reached 9% or 30% respectively, whereas the weight percent fraction of PFOB (the loaded agent) represented 69% or 43% of the total microcapsule weight. The mean sizes were  $41.50 \pm 0.68 \mu\text{m}$  and  $6.41 \pm 0.02 \mu\text{m}$  respectively. The  $D_{90}$  value (90% of the particles are smaller than this diameter) was significantly lower for the microcapsules synthesized at basic pH than for the ones synthesized at neutral pH, indicating a narrower distribution of the microcapsule size. Additionally, the yield of microcapsules decreased when reducing the temperature from 30°C to 20°C.

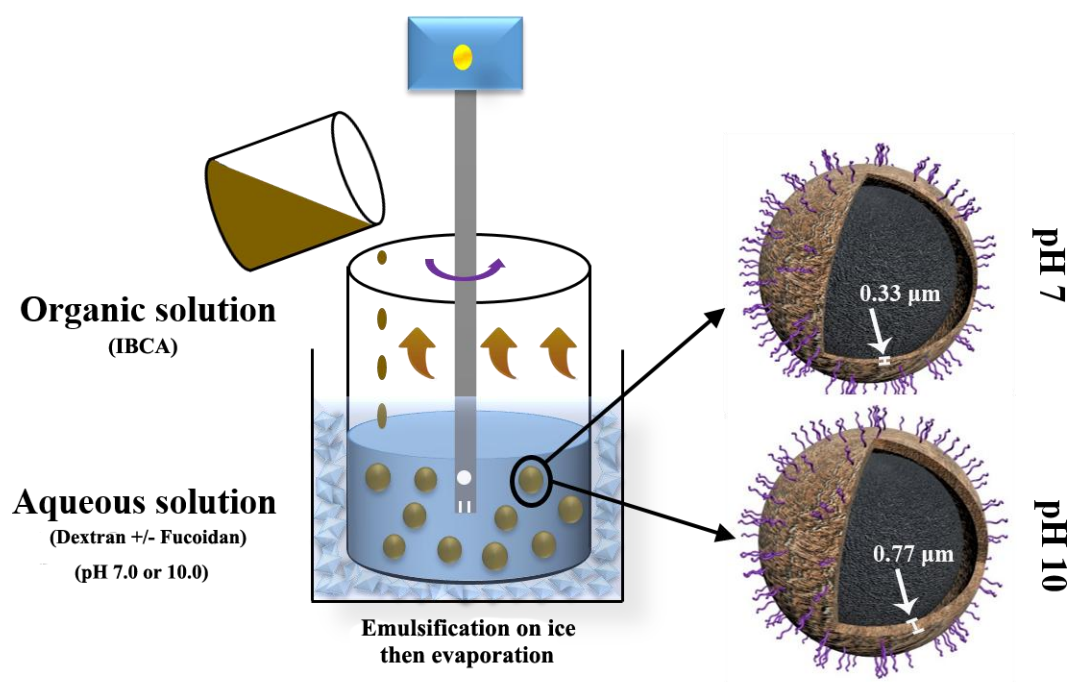


**Figure 1.** Overall scheme of one-step protocol for microcapsules synthesis.

**Table 1.** Characteristics of non-functionalized microcapsules.

pH	T (°C)	Polysaccharide	Stability in water	Size distributions			Zeta potential	Yield	Loaded agent
				D <sub>10</sub> (μm)	D <sub>50</sub> (μm)	D <sub>90</sub> (μm)	ζ (mV)	(%, w/w)	(%, w/w)
3	30	Dextran	No product	-	-	-	-	-	-
7	30	Dextran	Stable	1.57±0.01	5.68±0.04	41.50±0.68	-16.83±0.31	9.00±2.15	69.02±3.44
10	30	Dextran	Stable	2.40±0.01	4.07±0.01	6.41±0.02	-12.10±0.59	30.03±1.98	42.54±2.16
10	20	Dextran	Stable	2.31±0.04	4.03±0.05	6.50±0.10	-16.25±0.42	25.88±2.70	42.50±1.68

To further visualize the polysaccharide presence in microcapsules, a portion of dextran (1% w/w) was substituted during the emulsion process by FITC-dextran, and Nile red was added in the organic phase to stain in red the hydrophobic poly (isobutyl cyanoacrylate) (PIBCA). Microcapsule suspensions were observed by confocal microscopy (**Figure 2 Left**). The core–shell structure of the microcapsules was perfectly visible; the core composed of liquid appeared in dark and the fluorescent shell was well defined. Surprisingly, polysaccharides were not preferentially localized at the polymer/water interface. In fact, the green fluorescence was homogeneously distributed in the whole shell thickness, the polysaccharides being therefore mixed with the polymer shell.

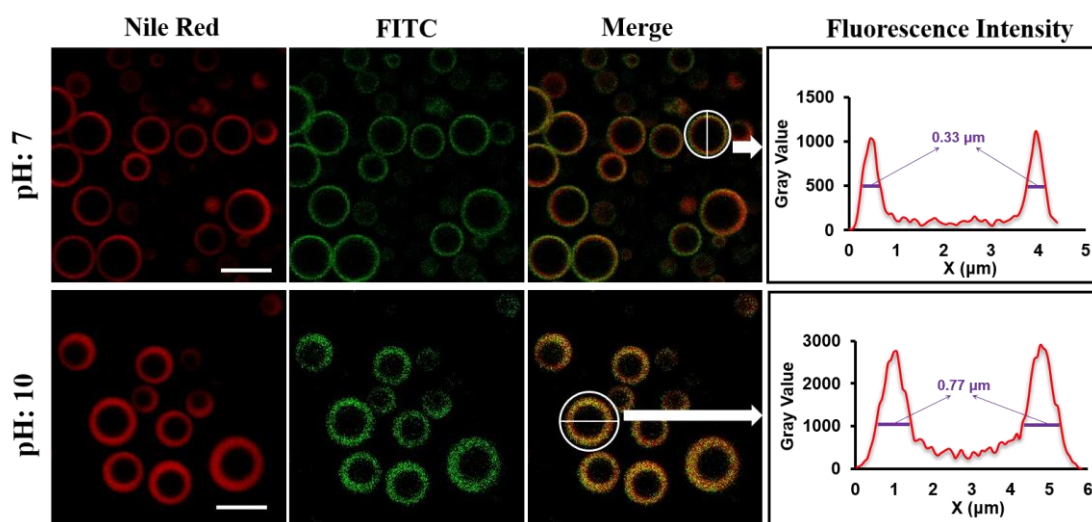


**Figure 2.** Confocal microscopy images of microcapsules (**Left**). Polymers appeared in color and the liquid content appeared in dark.

Red fluorescence channel: PIBCA (left), green fluorescence channel: FITC-Dextran (center) and merging of both channels (right), pH 7 (top), pH 10 (bottom) (Scale bar = 5  $\mu\text{m}$ ). Fluorescence Intensity graph profile (X: distance measurement) (**Right**). Determination of the shell thickness, pH 7 (top) and pH 10 (bottom). (n=3)

The scanning of focused equatorial slice of Nile red-labeled microcapsule shells was performed and the fluorescence intensity profiles were measured (**Figure 2 Right**). Confocal images showed that microcapsules had a thickness of  $0.33 \pm 0.08 \mu\text{m}$  and  $0.77 \pm 0.13 \mu\text{m}$  for reaction medium pH of 7 and 10 respectively.

To obtain functionalized particles, fucoidan was introduced into the polymerization medium, as 10% w/w of the total polysaccharide mass. As indicated in **Table 2**, stable microcapsules functionalized with fucoidan (Fuco-MCs) had a mean size of  $7.09 \pm 0.14 \mu\text{m}$ . The zeta potential of Fuco-MCs decreased compared to MCs ( $-50.88 \pm 0.52 \text{ mV}$  vs  $-12.10 \pm 0.59 \text{ mV}$  for MCs). This result indicated that at least a part of the anionic fucoidan was present at the surface of the microcapsules, a property already observed with fucoidan coated nanoparticles<sup>[23]</sup>. To further evidence the presence of fucoidan in Fuco-MCs, FITC-fucoidan (1% w/w of the total fucoidan mass) was incorporated during their synthesis. The co-localization of FITC-fucoidan and the microcapsules was evaluated by flow



cytometry. Non-fluorescent Fuco-MCs were used as a control to adjust their autofluorescence level. A noticeable difference in the fluorescent signal was detected between FITC-Fuco-MCs and Fuco-MCs, indicating that almost all microcapsules in contact with FITC-fucoidan were functionalized by FITC-fucoidan (**Figure 3**).

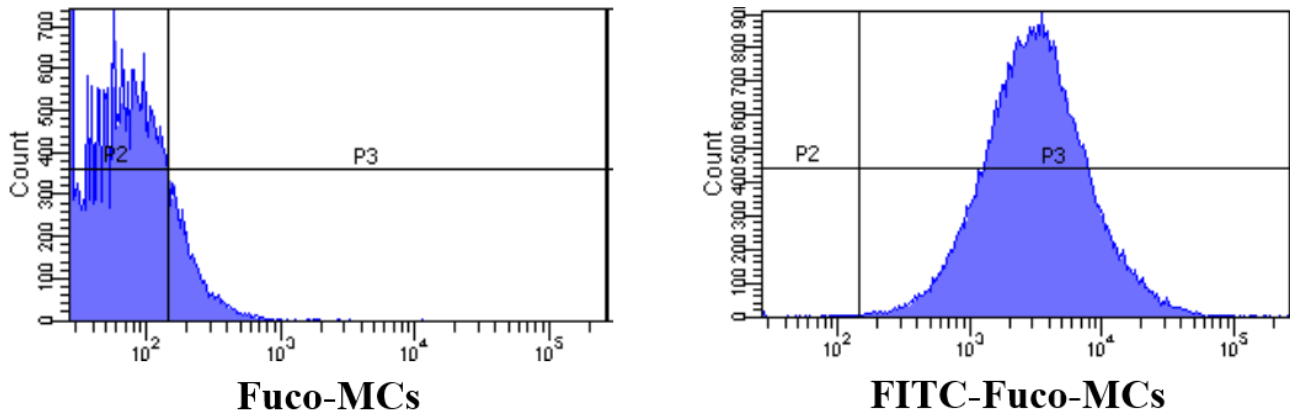


**Figure 3.** Flow cytometry evaluation of the co-localization of FITC-Fucoidan with microcapsules. 1% w/w of FITC-fucoidan was introduced during the synthesis of Fuco-MCs. The green fluorescence signal associated to the fucoidan functionalized microcapsules was analyzed by flow cytometry in presence or not of FITC-fucoidan.

**Table 2.** Characteristics of non-functionalized and functionalized microcapsules.

Microcapsules	Stability in water		Size distributions			Zeta potential	Yield	Loaded agent
			D <sub>10</sub> (μm)	D <sub>50</sub> (μm)	D <sub>90</sub> (μm)	ζ (mV)	(%, w/w)	(%, w/w)
Non-functionalized (MCs)	Stable	After preparation	2.40±0.01	4.07±0.01	6.41±0.02	-12.10±0.59	30.03±2.12	42.54±3.05
		After purification	2.24±0.02	3.79±0.03	5.90±0.10	-8.86±0.88	29.25±3.48	42.05±2.56
Functionalized with fucoidan (Fuco-MCs)	Stable	After preparation	2.30±0.01	4.19±0.05	7.09±0.14	-50.88±0.52	28.51±2.61	45.86±1.98
		After purification	2.19±0.02	3.69±0.02±	5.84±0.05	-51.76±1.33	24.56±3.11	41.15±2.87

The size distribution of each type of microcapsules decreased after purification. After purification, both MCs and Fuco-MCs had similar size distribution (from 2.2  $\mu\text{m}$  to 5.9  $\mu\text{m}$  for MCs and from 2.2  $\mu\text{m}$  to 5.8  $\mu\text{m}$  for Fuco-MCs) and the mass percent of loaded agent was similar (42% and 41% respectively) (**Table 2**).

The morphology of obtained microcapsules was analyzed by Scanning Electron Microscopy (SEM) and Transmission Electron Microscopy (TEM) (**Figure 4**). Both MCs and Fuco-MCs showed a typical well-defined spherical capsule structure.

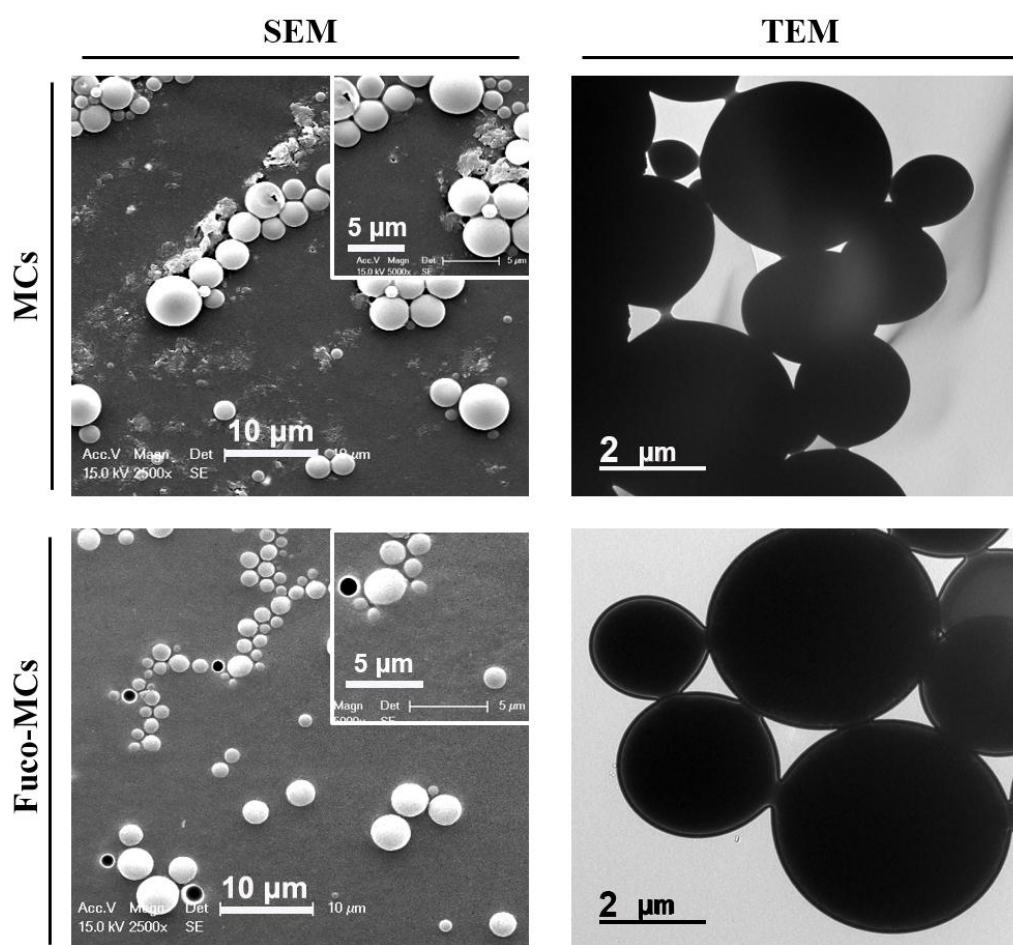


**Figure 4.** Scanning and Transmission Electron Microscopy images of microcapsules. Top: MCs. Bottom: Fuco-MCs. Left: SEM images with zooms. Right: TEM images.

Quantitative analysis showed that Fuco-MCs contained 0.10  $\mu\text{mol/g}$  of sulfur. Since the fucoidan used in this study was determined to contain 1,550  $\mu\text{mol/g}$  of sulfur, we calculated the fucoidan

content of Fuco-MCs to be 0.008 % (w/w) right after synthesis. Long-term stability in distilled water was assessed upon storage of the suspensions at 4°C. Size and zeta potential remained stable at least one month for both types (**Figure. 5**). Moreover, the content of fucoidan in Fuco-MCs did not obviously change with time (0.006 % (w/w) at 1 month).

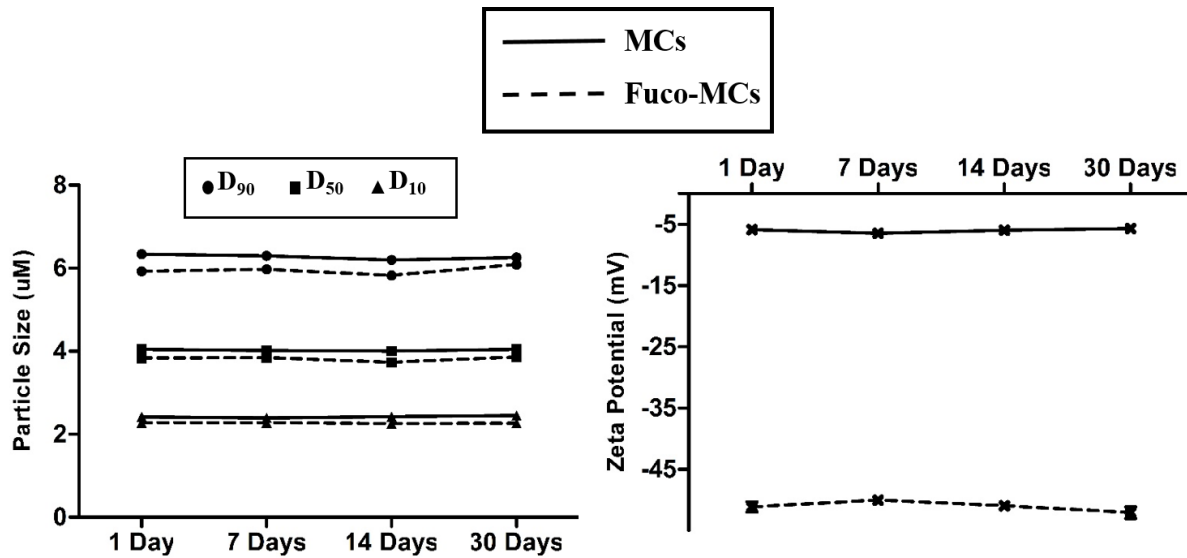


**Figure 5.** Stability at 4°C in distilled water of MCs and Fuco-MCs suspensions according to size and zeta potential measurements.

## 2.2. Static binding on platelets

To evaluate the affinity of MCs and Fuco-MCs for P-selectin expressed onto the surface of human activated platelets, flow cytometry experiments were performed. Interactions were assessed between microcapsules and three groups respectively composed of: human Plasma-Rich Platelets (PRP), human Plasma-Rich Platelets where platelets were activated with TRAP (PRP+TRAP), and human Plasma-Rich Platelets where platelets were activated with TRAP and P-selectin blocked by a specific blocking antibody (PRP + TRAP + anti-CD62P). As shown on **Figure 6**, non-functionalized microcapsules (MCs) barely or only minimally bound to the three groups of platelets, as shown by low values of the mean fluorescence intensity (MFI) ( $9.75 \pm 2.11$ ;  $9.00 \pm 0.87$ ;  $6.50 \pm 1.77$ , respectively). In contrast, Fuco-MCs exhibited an important binding to activated platelets (MFI = 12

$008 \pm 2\,359$ ) compared to PRP (MFI =  $432.4 \pm 212.8$ ) or to PRP + TRAP + anti-CD62P (MFI =  $1093 \pm 419.2$ ).

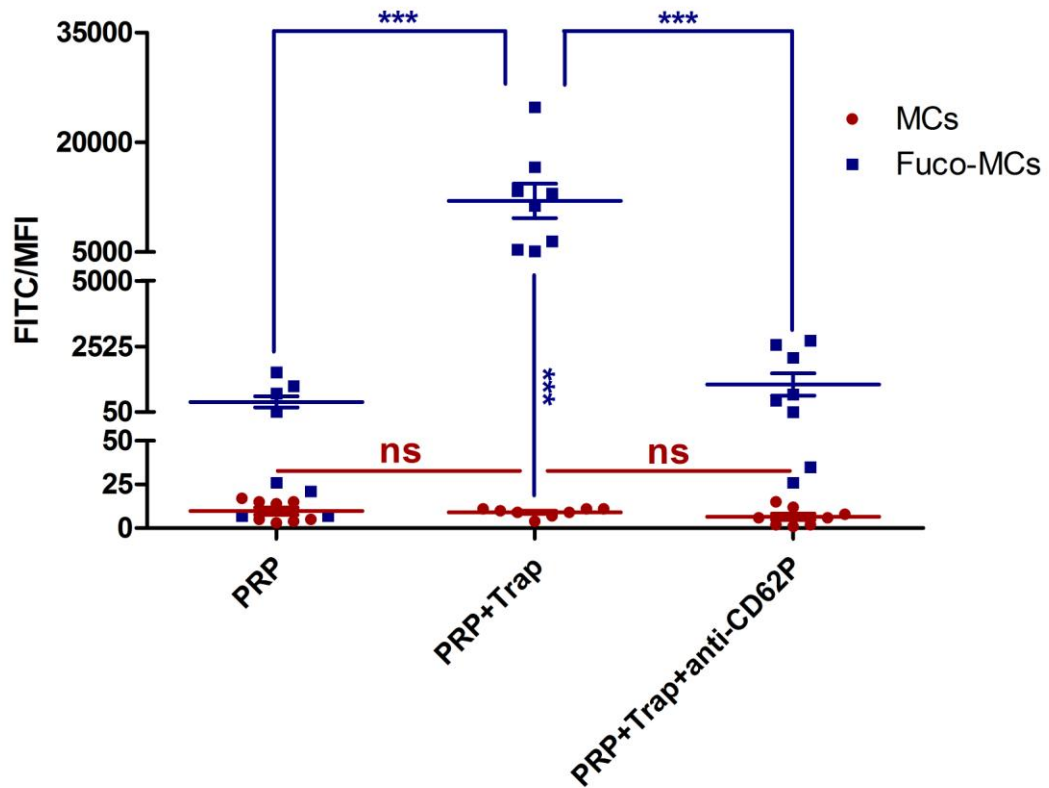


**Figure 6.** Flow cytometry assessment of interactions of FITC-labeled MCs and FITC-labeled Fuco-MCs with either non-activated platelet-rich plasma (PRP), platelet-rich plasma activated with TRAP (PRP+Trap) and platelet-rich plasma activated plus P-selectin antibody (PRP+Trap+anti-CD62P). The mean fluorescence intensity (MFI) on the FITC channel was measured for 50,000 events of PE-Cy5 labeled platelets, and at a microcapsule concentration of 50 g/L (n=8; \*\*\*p<0.001).

### 2.3. Flow chamber experiments

To evaluate the ability of MCs and Fuco-MCs to target selectins under arterial blood flow conditions, flow chamber experiments with selectins coating were performed. Under arterial blood flow, FITC-Fuco-MCs showed a significantly higher adhesion to P-selectin than FITC-MCs ( $5565 \pm 662$

adhered Fuco-MCs versus  $482 \pm 113$  adhered MCs,  $p < 0.001$ ) (**Figures 7 A&D**). Fuco-MCs adhered to the chamber immediately after their injection and remained attached for the whole duration of the experiment. On the contrary, only few MCs were seen to adhere. Washing with NaCl 0.9% at the end of the experiment did not significantly affect the adhesion of both types of microcapsules. The number of adhered Fuco-MCs after 5 min was significantly lower to E-selectin ( $854 \pm 502$ ) or L-selectin ( $10 \pm 8$ ) than to P-selectin ( $5565 \pm 662$ ) (**Figure 7A**). Adhesion of Fuco-MCs was comparable to that of MCs on E-selectin or L-selectin.

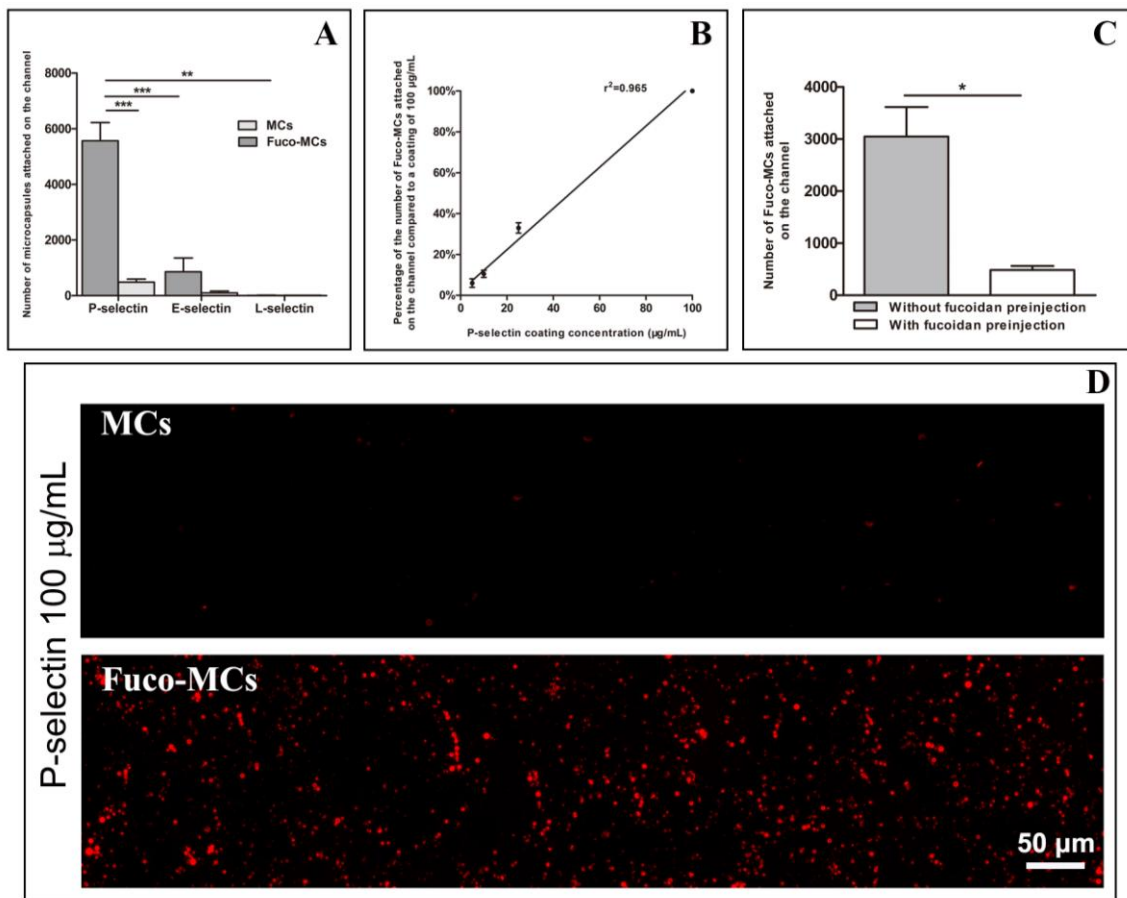


**Figure 7.** Evaluation of microcapsule interactions with recombinant selectins in an *in vitro* arterial flow assay. **A)** Adhesion of microcapsules on selectins. Channels were coated at an E, L, P-selectin concentration of 100  $\mu\text{g/mL}$ . MCs and Fuco-MCs were injected over 5 minutes under arterial flow conditions (shear rate:  $1,500 \text{ s}^{-1}$ ). After 5 minutes, channels were washed with 0.9% NaCl. The number of fluorescent microcapsules attached along each channel was quantified with Histolab (Microvision) ( $n > 3$ ,  $**p < 0.01$ ,  $***p < 0.001$ ). **B)** Number of attached microcapsules as a function of the P-selectin concentration from 5  $\mu\text{g/mL}$  to 100  $\mu\text{g/mL}$ . The

number of microcapsules was normalized over the average number of microcapsules attached for a P-selectin concentration of 100  $\mu\text{g/mL}$ . **C)** Fucoidan pre-injection inhibits Fuco-MCs binding. Channels were coated at a P-selectin concentration of 100  $\mu\text{g/mL}$ . After washing with 0.9% NaCl, fucoidan solution (10 mg/ml) was injected or not over 5 min, then microcapsules were injected during 5 minutes. Channels were washed and the number of microcapsules was quantified (\* $p < 0.05$ ). **D)** Macroscopic view of MCs or Fuco-MCs adhesion over a P-selectin coating of 100  $\mu\text{g/mL}$ . (n=10 for MCs and n=11 for Fuco-MCs; Scale bar = 50  $\mu\text{m}$ ).

The Fuco-MCs adhesion dependence on P-selectin concentration was investigated (**Figure 7B**). The number of attached Fuco-MCs was normalized over the mean number of attached microcapsules for a P-selectin concentration of 100  $\mu\text{g/mL}$ . Results indicated a dose-dependent relation between the concentration of P-selectin and Fuco-MCs ( $r^2 = 0.965$ ) (**Figure 7B**). The competitive inhibition experiments showed that the injection of a free fucoidan solution (10 mg/ml) before the injection of Fuco-MCs suspension inhibited the binding of Fuco-MCs to P-selectin ( $486 \pm 75$  versus  $3048 \pm 565$ , respectively,  $p < 0.05$ ) (**Figure 7C**).

To mimic the interaction of microcapsules and P-selectin under physiological conditions, human platelets from whole blood were activated and aggregated on collagen at high shear stress (67.5  $\text{dyn/cm}^2$ ). Aggregating platelets were visualized in real time under phase contrast microscopy and expression of P-selectin was evidenced by the green fluorescence uptake after injection of a FITC anti-CD62P antibody through the channel (**Figure 8A**). No signal was detected after injection of the FITC-IgG control (Data not shown). When passed at arterial flow on the platelets aggregates, Fuco-MCs bound to the aggregates and remained attached, whereas MCs showed almost no binding (**Figure 8A**). Quantitative analysis after 5 minutes confirmed that the mean fluorescence intensity of fluorescent microcapsules was significantly higher for Fuco-MCs than for MCs ( $2275 \pm 188$  MFI versus  $305 \pm 69$  MFI, respectively,  $P < 0.001$ ) (**Figure 8B**).

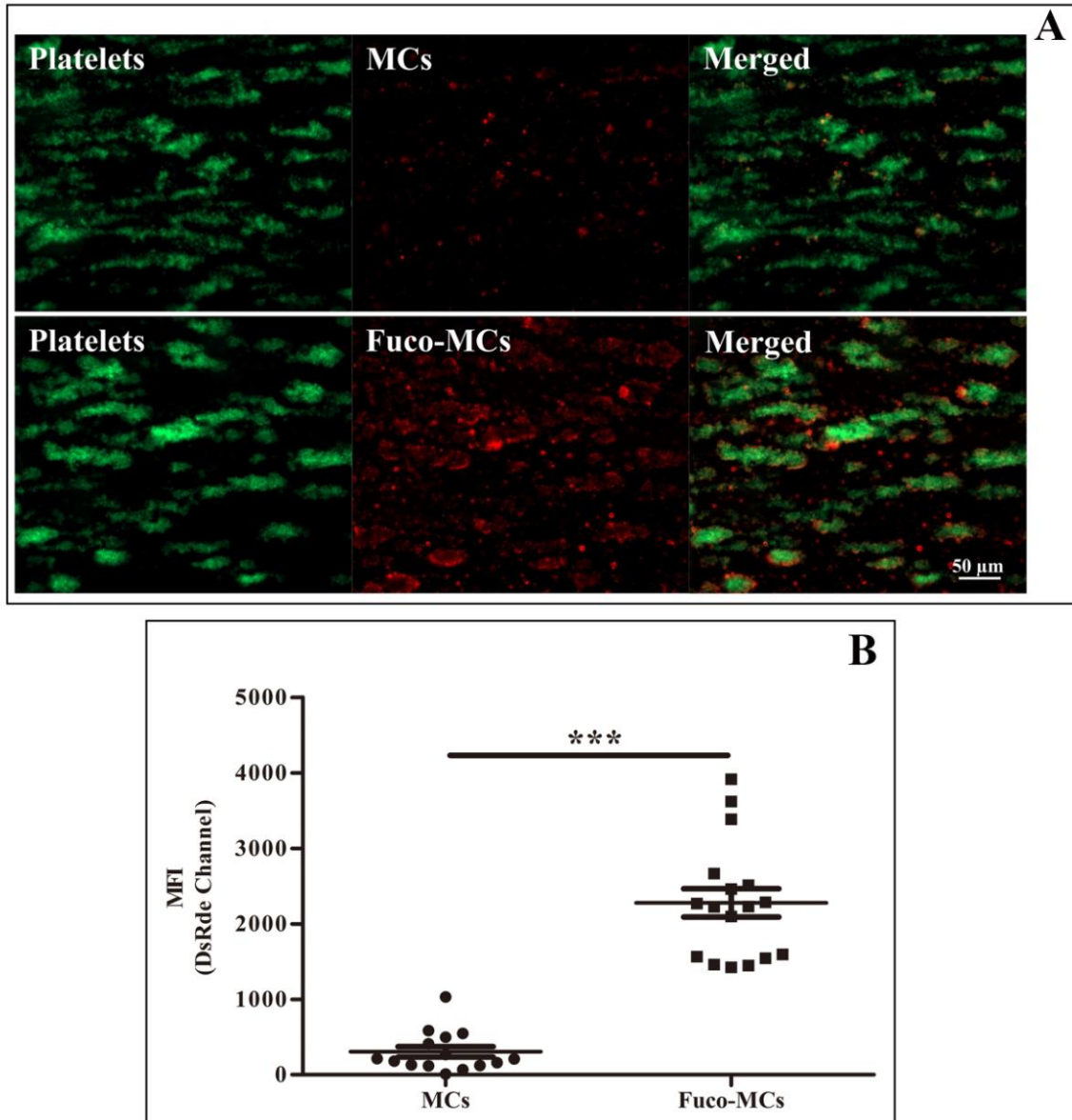


**Figure 8.** Microcapsule adhesion over platelet aggregates. **A)** Whole blood labeled with Dioc6 was injected onto channels coated with collagen at 50  $\mu$ g/mL. Under arterial flow conditions, platelets adhered onto the channel wall forming aggregates expressing P-selectin (Left) and FITC-MCs or FITC-Fuco-MCs were then injected for 5 minutes (Middle panel). Channels were washed with 0.9% NaCl. Microcapsules and aggregates co-localization was assessed by merged fluorescence microscopy (Right). **B)** Quantitative analysis of the mean fluorescence intensity of platelet aggregates (n=15 for MCs and n=17 for Fuco-MCs; \*\*\*p<0.001).

## 2.4. Cell viability

The cytotoxicity of microcapsules was evaluated by MTT assay. As shown in **Figure 9**, the results demonstrated that MCs and Fuco-MCs did not significantly affect the mean viability of mouse

fibroblasts 3T3 cells at concentrations of 0.625, 1.25, 2.5 and 5 g/L, there were no obvious difference between MCs and Fuco-MCs.

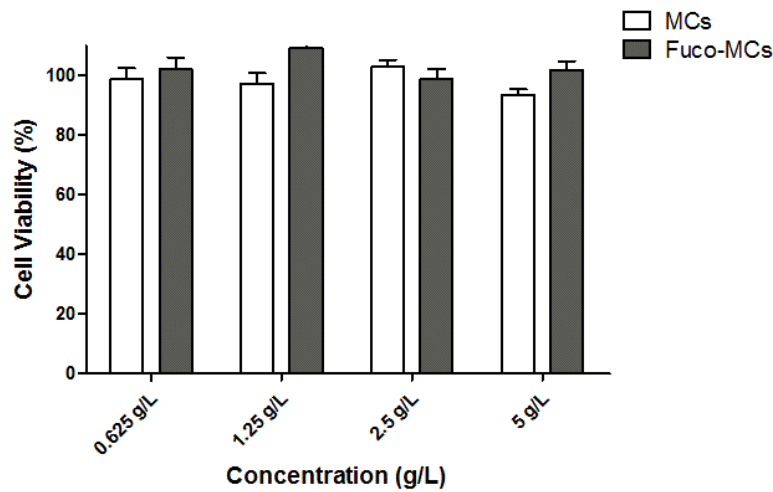


**Figure 9.** MTT assay performed on 3T3 cells after 24 h of incubation in the presence of MCs and Fuco-MCs at different concentrations.

(n=6)

## 2.5. Localization of microcapsules within the thrombotic Abdominal Aortic Aneurysm wall of rats and biodistribution

To assess whether Fuco-MCs accumulated *in vivo* within an AAA, histological staining of both AAA and healthy aorta samples were performed 1 hour after the injection of FITC-MCs and FITC-Fuco-MCs. On histological stained sections, smooth muscle cells from connective tissues and several layers of the aneurysmal wall were distinguished (**Figure 10A**). Many Fuco-MCs (red spheres) were localized in the arterial wall, between the thrombus and the media layer compared to MCs (**Figure 10A**). On the other hand, only few Fuco-MCs were found in arterial wall of healthy rats (**Figure 10A**). Semi-quantitative analysis confirmed that the fluorescence in the AAA wall was higher for Fuco-MCs than for MCs, and the binding of Fuco-MCs or MCs in healthy aorta was low (**Figure 10B**).

To evaluate the biodistribution, the presence of MCs and Fuco-MCs in four organs (liver, spleen,



lungs and kidneys) was assessed at 1 hour and 24 hours after injection by histological analysis of several sections of each organ. At 1 hour, both types of microcapsules were mainly found in lungs, (although no respiratory problems were noted), then in liver, in spleen and finally in kidneys. At 24 hours, the number of microcapsules decreased in a similar way in the four organs.

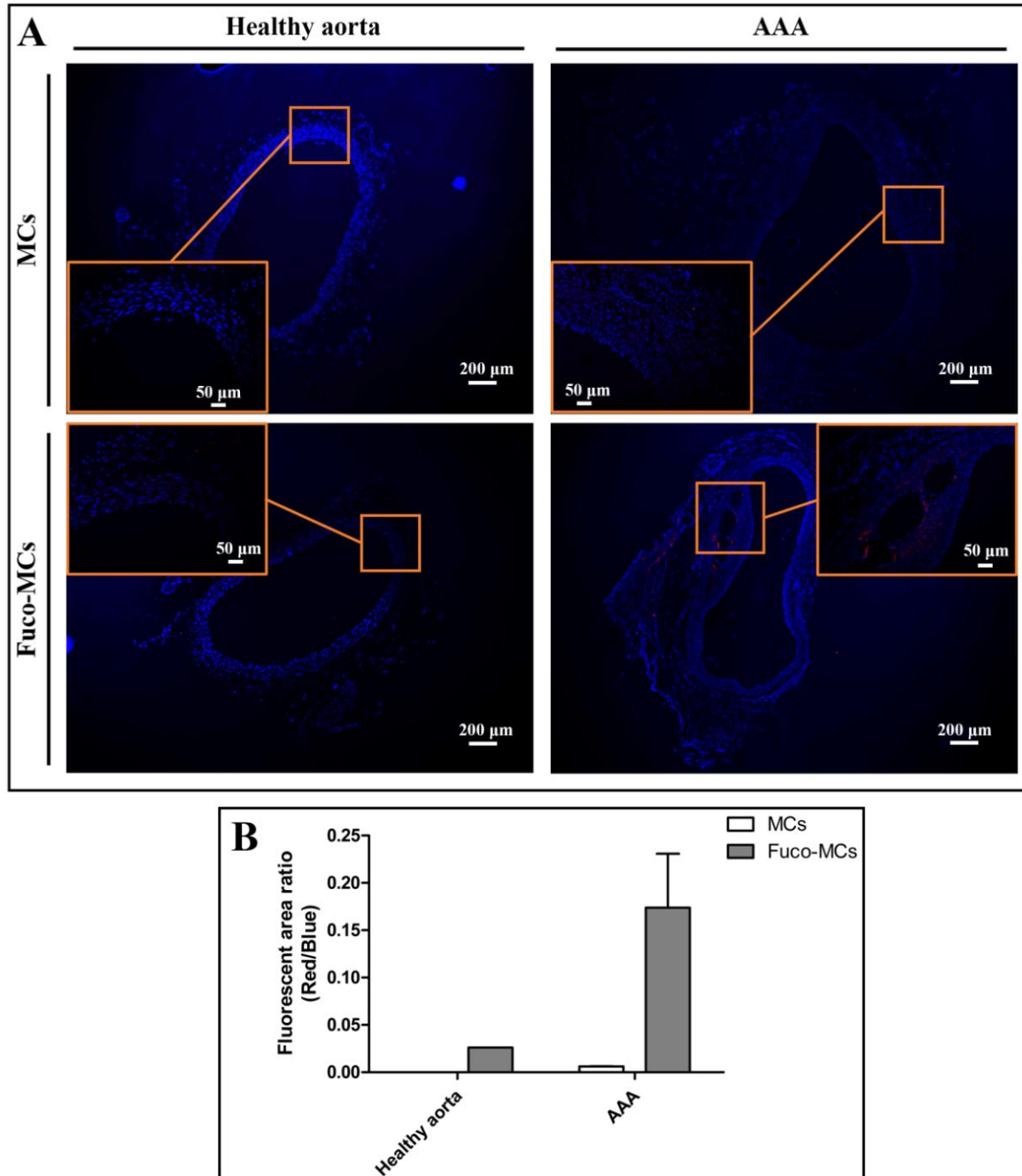


**Figure 10.** Histological analysis of abdominal aorta sections (A). Healthy rats (left) and rat Abdominal Aorta Aneurysms (right).

Inserts are magnification of Regions of Interest. Muscle cells appear in blue fluorescence and MCs or Fuco-MCs appear in red.

Semi-quantitative analysis of histological sections (B). Data are expressed as the proportion of red fluorescent area to blue fluorescent area (x20) on healthy rats or rats with AAA injected with MCs or Fuco-MCs.

### 3. Discussion

In this study, injectable core-shell polymer microcapsules functionalized with fucoidan were developed as a carrier tool to target P-selectin overexpressed in cardiovascular diseases.

Nanoparticle made of PACA and coated with polysaccharides are promising substrates because of their biodegradability and biocompatibility.<sup>[10, 24]</sup> We developed here microcapsules composed of a lipophilic liquid core and a PIBCA-polysaccharide mixed membrane. This microcapsule structure was prepared by a new emulsion-evaporation polymerization process performed either in neutral or alkaline conditions. Using this method, the rate of polymerization was controlled by the evaporation rate. This technique allowed for the first time the polymerization of IBCA in emulsion under neutral and alkaline conditions leading to reproducible polymer microcapsules that can be functionalized with polysaccharides such as fucoidan.

Two key conditions must be fulfilled to form stable core-shell microcapsules. First, the water phase should contain water-soluble colloidal stabilizers, such as polysaccharides, making microcapsules more hydrophilic and avoiding particle aggregation. Second, the pH of the polymerization medium should be well controlled. Acidic condition reduced the initial polymerization rate resulting in insufficient polymer film thickness which did not provide enough surface tension to make droplets. Under neutral or alkaline conditions, the hydroxyl ions in the solution could accelerate the polymerization reaction to form stable shell encapsulating a hydrophobic agent.

For the use as drug carriers, the shell thickness-to-radius ratio (T/R) strongly influenced the embedded drug release behavior. Jiao *et al.* showed that the amount and rate of doxorubicin release in hollow mesoporous silica nanoparticles exhibited shell thickness dependence, decreasing with the increase of the shell thickness.<sup>[25]</sup> Furthermore, compare to undesired burst effect, drug controlled release prolongs the time of drug action.<sup>[26]</sup> Interestingly, we found that the polymer thickness could

be easily modified from 330 nm to 770 nm depending on the pH of the polymerization medium. This property could be optimized for controlled drug release. In this study, PFOB was used as a reference agent. The theranostic potential of these microcapsules will be investigated in the near future.

As previous studies, we found that Fuco-MCs shown low value of zeta potential compare to MCs. Flow cytometry experiments demonstrated that microcapsules were functionalized by fucoidan. Although the weight content of fucoidan in microcapsules was very low, it was stable at least for one month without obvious release. SEM and TEM analysis along with size measurements showed that the functionalization of microcapsules with fucoidan did not affect the spherical shape or the diameter distribution. Charoenphol *et al.* indicated that spheres exhibiting a diameter of 2.5  $\mu\text{m}$  are optimal for targeting purposes in medium to large vessel walls, which are affected in numerous cardiovascular diseases.<sup>[3, 27]</sup> The size of our microcapsules from 2.2  $\mu\text{m}$  to 5.8  $\mu\text{m}$  appeared therefore adapted for vascular targeting purposes.

Cell viability assay is a powerful tool in providing valuable information regarding the safety of biomaterials. In this study, the *in vitro* cytotoxicity of microcapsules was evaluated by a colorimetric MTT assay on reference 3T3 cells. Results indicated that both types of microcapsules did not present obvious detrimental effects on 3T3 cells proliferation even at high concentration. Moreover, there was no significant difference between MCs and Fuco-MCs, as both of them had no cytotoxicity and good biocompatibility.

Using flow cytometry, we evidenced that the Fuco-MCs exhibited a stronger affinity for human activated platelets than MCs and that this binding could be inhibited by a P-selectin antibody. Similar results had been published by Bonnard T. *et al.* using fucoidan functionalized polysaccharide microparticles.<sup>[28]</sup>

Up to now, the design of carrier systems targeting specific molecules and able to bind them under

high velocity blood flow conditions remains a challenge. In this study, an *in vitro* flow adhesion assay onto recombinant selectins confirmed that fucoidan functionalized microcapsules/Fuco-MCs rapidly and specifically bound to P-selectin compared to MCs even under high shear rate conditions (1,500 s<sup>-1</sup>). Moreover, the number of attached Fuco-MCs was dependent on P-selectin concentration and free fucoidan in solution inhibited the binding of Fuco-MCs to P-selectin. Previous reports indicated that the sulfate ester groups of fucoidan could be recognized by P-selectin and L-selectin,<sup>[29]</sup> but not by E-selectin.<sup>[30]</sup> Our results indicated that Fuco-MCs could bind P-selectin but not L-/E-selectins. Moreover, Fuco-MCs revealed a higher ability as compared to MCs to adhere to the surface of activated platelet aggregates under arterial flow conditions. The interaction between the fucoidan coated onto microcapsules and the P-selectin was strong enough to overcome kinetic energy of microcapsules even with their high density (close to 1.3 g/mL) that comes from the presence of liquid PFOB into their core.

Histological and semi-quantitative analysis revealed that Fuco-MCs were localized inside the media layer of the thrombotic AAA wall in rats, whereas very low binding was observed on AAA injected with MCs or on the artery wall of healthy rats injected with Fuco-MCs. Biodistribution studies showed that both types of microcapsules were present in the Mononuclear Phagocyte System (MPS), which is consistent with what is described in the literature, that they tended to be eliminated over 24 hours and that they had no adverse effect on the health of rats. In fact, some of the injected rats were still alive after 3 months. Since microcapsules functionalized with fucoidan accumulated in the inner wall of the AAA, a promising strategy to treat AAA could be to inhibit the proteolytic activity which occurs within the medial layer and lead to the arterial wall degradation.<sup>[31]</sup> The ability of Fuco-MCs to target the AAA could be associated with the loading of a proteolytic inhibitor in this microcarrier. Preliminary *in vitro* experiments also indicated that the loading of microcapsules with PFOB allowed

ultrasound imaging. Such microcapsules loaded with a drug and functionalized with fucoidan appear therefore as promising molecular theranostic systems.

#### **4. Conclusions**

Microcapsules functionalized with fucoidan were developed here for the targeting of activated platelets in thrombotic abdominal aorta aneurysm using biodegradable and biocompatible polymer membrane composed of poly(isobutyl cyanoacrylate) and polysaccharides. In this work, we described their elaboration with a new alkaline solvent emulsion-evaporation polymerization process and we confirmed their hydrodynamic diameter distribution, the microcapsule structure and the presence of the targeting agent, fucoidan, at the surface. This work gave the first evidence that functionalized microcapsules can be obtained according to an easy one-step polymerization process of isobutyl cyanoacrylate in neutral and alkaline conditions. *In vitro* cytotoxicity assay showed that the microcapsules exhibited excellent compatibility with cells *in vitro*. Subsequently, we demonstrated *in vitro* by flow cytometry that these fucoidan functionalized microcapsules could specifically bind to the P-selectin expressed by human activated platelets. Flow chamber experiments further confirmed that Fuco-MCs bind to P-selectin and to activated platelet aggregates even at high shear rate. Finally, we showed *in vivo* on rats the ability of Fuco-MCs to bind to thrombotic AAA and evidenced their presence in the AAA wall by histology. Future works are required to study the loading of contrast agents or therapeutics to achieve molecular diagnosis and/or treatment of cardiovascular pathologies overexpressing P-selectin.

#### **5. Experimental Section**

*Materials:* Methylene chloride ( $\text{CH}_2\text{Cl}_2$ ) RPE-ACS 99.5% and Acetone 99.8% were provided by Carlo Erba Reactifs (Peypin, France). 1-Bromoheptadecafluorooctane (PFOB),  $\text{CDCl}_3$  (99.96 atom % D), isopropanol, MTT solution and Nile Red were provided by Sigma Aldrich (Saint Quentin Fallavier, France). Dextran 20 and FITC-Dextran 20 were obtained from TdB Consultancy (Uppsala, Sweden). Fucoidan was a gift from Algues & Mer (Ouessant, France). Perfluoro-15-crown-5-ether (PFCE) was purchased from Fluorochem (Hadfield, UK). Isobutyl cyanoacrylate (IBCA) was provided by ORAPI (Saint Vulbas, France). TRAP (thrombin receptor-activating-peptide) was obtained from PolyPeptide laboratories (Strasbourg, France). PE-Cy<sup>TM</sup>5 mouse anti-human CD41a and PE-Cy<sup>TM</sup>5 mouse IgG1, $\kappa$  Isotype Control were provided by BD Pharmingen, (Le Pont-de-Claix, France), mouse anti-human CD62P, mouse anti-human CD62P-FITC and mouse IgG1-FITC Isotype Control were obtained from Beckman Coulter (Villepinte, France). Recombinant human E-selectin, L-selectin and P-selectin were provided by R&D Systems (Lille, France). Flow chambers (Vena8Fluoro+) were obtained from Cellix Ltd (Dublin, Ireland).

*Synthesis of core-shell microcapsules:* Dextran 20 coated poly(isobutyl cyanoacrylate) (PIBCA) microcapsules (MCs) with 1-Bromoheptadecafluorooctane (PFOB) core as a reference loaded agent were prepared by modification of the emulsion-evaporation process described by Pisani.<sup>[32]</sup> Briefly, 100  $\mu\text{L}$  of IBCA was dissolved into 4 mL of methylene chloride along with 60  $\mu\text{L}$  of PFOB. The organic solution was mixed to ensure full miscibility of the PFOB. Subsequently, the whole organic phase was slowly injected into 20 mL of a cold aqueous solution containing 300 mg of dextran (1.5% (w/v)) adjusted to the desired pH conditions (pH 3, 7 or 10), and dispersed at 30,000 rpm for 2 min with a homogenizer (Polytron PT 3100, dispersing aggregate PT-DA 07/2 EC-B101, Kinematica, Luzern, Switzerland). To prepare fucoidan-functionalized microcapsules (Fuco-MCs), 30 mg of fucoidan was blended into 270 mg of dextran. They were dissolved into an aqueous solution at pH 10.

Emulsification was performed in a 50 mL beaker placed in ice. Methylene chloride was then evaporated by magnetic stirring for about 4 h at room temperature or 3 h in a thermostated bath (30°C). After full evaporation of the solvents, samples were centrifuged at 600 g for 30 min (5702RH centrifuge Beckman Coulter, Villepinte, France), supernatants were discarded and precipitates were washed by deionized water. The centrifugation and washing steps were repeated three times. For fluorescent and confocal microscopy studies, 10 µL (0.57 mg/ml) of Nile red were added to the organic solution and 3 mg of FITC-dextran were added to the aqueous solution before emulsification. The fluorescence intensity of microcapsules was analyzed by Image J software. Finally, the precipitate was resuspended into 3 mL of deionized water for storage at 4°C until use or for freeze-drying.

For freeze-drying, the purified suspensions were frozen at -18°C and freeze-dried during 48-72 h without using any cryo-protecting agent (Lyovac, SRK Systemtechnik, Riedstadt, Germany).

The mass yield (%) was calculated as follows:

$$Yield = \frac{m_{Microcapsules}^{mass}}{m_{Polysaccharides}^{feed} + m_{polymer}^{feed} + m_{PFOB}^{feed}} \times 100\% \quad (1)$$

Where  $m_{Polysaccharides}^{feed}$ ,  $m_{polymer}^{feed}$ ,  $m_{PFOB}^{feed}$  are the initial masses of the components introduced in the reaction solution,  $m_{Microcapsules}^{mass}$  corresponds to the final mass of microcapsules evaluated after the freeze-drying process.

*Size and zeta potential microcapsule determination:* The size distribution of microcapsules was quantitatively obtained using a laser dynamic scattering granulometry at 25°C (Mastersizer 3000, Malvern Instruments, Orsay, France).

Zeta potential (ζ) of the microcapsules was measured to evaluate their stability in suspension and to identify the presence of the polysaccharides onto the surface. Samples were diluted in 1 mM KCl.

Measurements were performed at 25°C using quasi-elastic light scattering apparatus (Nano ZS, Malvern Instruments, Orsay, France).

All the measurements were performed in triplicate and the results were expressed as mean  $\pm$  standard deviation.

*Scanning Electron Microscopy (SEM) and Transmission Electron Microscopy (TEM):* The surface morphology of microcapsules was imaged using a Scanning Electron Microscopy apparatus (Philips XL 30 ESEM-FEG, Amsterdam, Netherlands) on dried samples coated with a thin gold layer. Transmission Electron Microscopy was performed using a Philips EM208 apparatus (Amsterdam, Netherlands) operating at 80 kV.

*Determination of PFOB content:* Microcapsules were freeze-dried for 24-48 hours. Subsequently, freeze-dried microcapsules were dissolved into  $\text{CDCl}_3$  along with PFCE as an internal standard ([PFCE] = 0.76 mmol/L). The  $^{19}\text{F}$  NMR (Nuclear Magnetic Resonance) spectra were recorded on a Bruker (400 MHz) Spectrometer (Billerica, USA). The amount of PFOB was obtained after integration of the peak at -80.7 ppm, corresponding to the  $\text{CF}_3$  group and normalization by the area of the PFCE peak at -89.5 ppm. Mass fraction  $C_{\text{PFOB}}$  was calculated as follows:

$$C_{\text{PFOB}} = \frac{m_{\text{PFOB}}^{\text{NMR}}}{m_{\text{MC}}} \quad (2)$$

Where  $m_{\text{MC}}$  is the quantity of freeze-dried microcapsules, and  $m_{\text{PFOB}}^{\text{NMR}}$  corresponds to the mass of PFOB recovered after the freeze-drying process.

*Sulfate and fucoidan quantification:* Sulfate quantification was conducted according to Gustaffson.<sup>[33]</sup> Briefly, a certain amount of fucoidan functionalized microcapsules was freeze-dried. Subsequently, the sample was exposed to nitrogen (100 mL/min) while boiled in iodohydric acid for 20 min. Released hydrogen sulfur reacted with zinc acetate (0.2 M) to form zinc sulfur. Then 8 mL of



ammonium iron sulfate at 16 mM and 2 mL of 3.7 mM diamine were added into the sample. Following 15 min of agitation, absorbance at 675 nm and 745 nm was measured using a spectrophotometer (PerkinElmer®). Sulfate content was calculated from a standard curve obtained with a potassium sulfate reference solution. Finally, sulfate content was measured and fucoidan content of the microcapsules was calculated.

*Static binding on platelets:* The interaction between three groups of PE-Cy5 labeled platelets (non-activated platelets (PRP), activated platelets (PRP + TRAP) and P-selectin blocked activated platelets (PRP + TRAP + CD62P) and two groups of microcapsules with FITC-dextran (MCs, Fuco-MCs) were measured by flow cytometry. 5 mL of blood from healthy adult volunteers were collected in sodium citrate 3.8% (w/v). Platelet-rich plasma (PRP) was obtained by centrifugation at 200 g for 15 min (5702RH centrifuge Beckman Coulter, Villepinte, France) and platelet concentration was adjusted to  $2 \times 10^8 \text{ ml}^{-1}$  with autologous platelet-poor plasma (PPP). Activated PRP was obtained by stimulation of PRP with 20  $\mu\text{M}$  TRAP (thrombin receptor-activating-peptide). In some experiments, activated then P-selectin-blocked PRP were obtained by incubation with a non-labeled anti-human CD62P at high concentration ( $0.04 \text{ g.L}^{-1}$ ). Before assessing the interaction with microcapsules, P-selectin expression level at the platelet surface was assessed using an anti-human CD62P-FITC. An additional tube of PRP was also incubated with a mouse IgG1/FITC to verify that the FITC signal was not due to non-specific binding to the platelets. In addition, MCs and Fuco-MCs were incubated with anti-human PE-Cy5 at a similar concentration to prove that microcapsules could not be labeled by antibody. Thus, for each test, we measured the FITC signal by flow cytometry and confirmed that P-selectin was expressed by platelets from PRP + TRAP batches and that low level of P-selectin was detected on PRP and PRP + TRAP + CD62P batches. To evaluate the binding ability between microcapsules with P-selectin expressed onto platelets, 5  $\mu\text{L}$  of

non-activated PRP, of activated PRP with TRAP or of anti P-selectin-treated activated PRP were incubated for 20 min with 5  $\mu$ l of MCs and of Fuco-MCs (50 mg/ml), together with 5  $\mu$ L of PE-Cy5 mouse anti-human CD41a to label platelets. In addition, each PRP sample was incubated with an isotype-matched control antibody. Samples were analyzed on a LSRII flow cytometer (BD Biosciences, Le Pont de Claix, France), 50,000 PE-Cy5 positive platelets collected per samples, and the mean fluorescence intensity (MFI) was measured in these platelets.

*Flow chamber experiments:* Channels were coated either with a solution of P-selectin, L-selectin or E-selectin at 100  $\mu$ g/mL (PBS). Some channels were coated with different concentrations of P-selectin (from 5  $\mu$ g/mL to 100  $\mu$ g/mL) to confirm that the affinity of Fuco-MCs for P-selectin was dependent on the concentration of P-selectin. The selectin solutions were left in the channels overnight at 4°C in a wet chamber. Channels were then washed with NaCl 0.9%. A suspension of fluorescent MCs or Fuco-MCs at 50 mg/mL in sterile saline was passed through the channels for 5 minutes at a shear rate of 1,500 s<sup>-1</sup>. For competitive binding experiment, fucoidan solution (10 mg/ml) was injected at the same rate 5 min before microcapsules were injected. After microcapsules injection, all the channels were washed with NaCl 0.9% for 1 minute at the same flow. Images of the bottom surface were taken along each channel. Fluorescence microscopy images were further analyzed with HistoLab software (Microvision, Evry, France) to quantify the number of attached particles.

For platelet dynamic binding experiments, channels were coated with collagen at 50  $\mu$ g/mL. The collagen solution was left in the channels overnight at 4°C in a wet chamber. Channels were then washed with NaCl 0.9%. Collagen fibers covering the channels wall were visualized by phase contrast microscopy. Human whole blood was passed through the channels for 3.5 minutes on average at 1,500 s<sup>-1</sup>. Platelets aggregations through contact with collagen were visualized in real time with phase contrast microscopy (Axio Observer, Carl Zeiss Microscopy, Oberkochen, Germany). The

channels were washed for 1 minute with NaCl 0.9%. On one channel FITC anti-CD62P antibody was infused at 20 µg/mL in NaCl 0.9% for a few minutes to confirm P-selectin expression on platelets membrane. One channel was used as a control for a control isotype-matched FITC-IgG at the same concentration. In the other channels, the platelets were labeled with Dioc6 (0.15 mM) before their injection. After their aggregation, fluorescent microcapsules (MCs or Fuco-MCs) were injected through the channels at 50 mg/mL for 5 minutes. Channels were finally washed for 1 minute with NaCl 0.9%. Images in phase contrast and in fluorescence microscopy were taken along each channel. Quantitative analysis was performed on at least three channels per type of microcapsules. The mean fluorescence intensity of the red fluorescence channel of several aggregates was measured using Zen 2012 Software (Carl Zeiss, Oberkochen, Germany). The red fluorescence background was measured on aggregates only and subtracted from the results.

*In vitro cytotoxicity:* To evaluate the cytotoxicity of the microcapsules and fucoidan functionalized microcapsules, MTT colorimetric assay was used on mouse fibroblasts 3T3 line. The cells were cultured in DMEM supplemented with 10% (v/v) fetal bovine serum (FBS), 4 mmol of L-glutamine, 100 units/mL of penicillin, and 100 µg/mL of streptomycin. The cells were kept in an incubator at 37°C in a humidified atmosphere of 5% CO<sub>2</sub>, 95% air. 3T3 cells were seeded (at the density of 10<sup>4</sup> cells per well) in 96-well plates (Costar) and incubated for 24 hours. After that, the cell culture medium was removed and 200 µL of series of dilution (0.625, 1.25, 2.5 and 5 g/L) of microcapsules in the medium were added to the plate. Culture medium were used as the positive controls. After 24 hour of incubation, the supernatant was removed and 10 µL (5 mg/mL) of MTT solution was added to the medium in each well and the plates were incubated for 4 hours at 37°C and 5% CO<sub>2</sub>. Then, the medium with MTT was removed and 100 µL per well of isopropanol solution was added to each well to dissolve the formazan crystals. The plates were read immediately in Tecan

(Infinite<sup>®</sup> M200 PRO) at 490 nm. The relative cell viability was expressed as Abs microcapsules/Abs control  $\times 100\%$ , where Abs control was obtained in the absence of the microcapsules.

*In vivo arterial disease model:* Animal studies were done in accordance with principles of laboratory animal care and with approval of the animal care and use committee of the Claude Bernard Institute (N°2012-15/698-0100) (Paris, France). The ability of the functionalized microcapsules to target P-selectin expression *in vivo* was assessed in an abdominal aortic aneurysm (AAA) experimental model in rats. The elastase model was performed on 8 male adult Wistar rats (7 weeks, Janvier Labs, Le Genest-Saint-Isle, France). Animals were anesthetized with intra-peritoneal injection of pentobarbital (1  $\mu\text{L/g}$  body weight, Ceva Santé Animale SA, La Ballastiere, France). Porcine pancreatic elastase (2.7 mg/mL, Sigma Aldrich, Saint Quentin Fallavier, France) was perfused into the lumen of an isolated segment of the infrarenal abdominal aorta for 15 minutes at a rate of 2.5 mL/h. Delbosc *et al.* reported that repeated intravenous injection of *Porphyromonas gingivalis* (Pg) in a rat model of AAA led to enhanced aortic dilation associated with neutrophil retention and persistence of a non-healing luminal thrombus.<sup>[34]</sup> In this study, *Porphyromonas gingivalis* suspension (107 CFU in 500  $\mu\text{L}$  0.9% saline), a gift from La Pitié Salpêtrière Hospital, was injected to the rats once a week via the penis vein for 4 weeks. Two days after the fourth injection, rats were anaesthetized by sodium pentobarbital intra-peritoneal injection (1  $\mu\text{L/g}$ ,) and 200  $\mu\text{L}$  of MCs or Fuco-MCs (50 mg/mL) in sterile saline were injected slowly via the penis vein. Healthy rats were injected as controls.

*Histology:* Animals were sacrificed with pentobarbital overdose 60 minutes after injection of MCs or Fuco-MCs. Abdominal aorta aneurysms of rats and healthy aorta of normal control rats were removed, washed in 0.9 % saline, fixed in paraformaldehyde (PFA) 4% (w/v) and then frozen. The aorta samples were cryo-sectioned at 10  $\mu\text{m}$  thicknesses for standard histology evaluations. The cell

nucleus of arterial vascular wall were labeled with DAPI, microcapsules expressed red fluorescence. The 20x magnified images of region of interest (ROI) were used for semi-quantitative analysis. The red and blue fluorescence areas were measured using ImageJ image analysis software.

Biodistribution of microcapsules were studied in a similar way. Briefly, liver, spleen, lungs and kidneys were excised and washed at 1 hour or 24 hours after injection of MCs or Fuco-MCs. The samples were cryo-sectioned and the cell nuclei were labeled with DAPI, the whole area of tissue slice of samples were used for semi-quantitative analysis.

*Statistical Analysis:* Data are presented as mean  $\pm$  SEM ( $n \geq 3$ ). Each experiment was performed using Student t test for paired data. Flow cytometry results were analyzed statistically with a one-way ANOVA with Bonferroni post-tests to compare data obtained with MCs and Fuco-MCs. A difference of  $P < 0.05$  was considered significant.

## Acknowledgments

This study was supported by Inserm, Paris Diderot University, Paris 13 University and Sorbonne Paris Cité. Bo LI is a recipient of the China Scholarship Council (CSC, No. 201206180031). The authors would like to thank C. Dong (CNRS UMR 7086, ITODYS, Paris Diderot University) for NMR measurements and F. Nadaud (UTC Compiègne, France) for SEM and TEM images. This work was also support by grants from ANR (ANR-12-EMMA-0020-01 “MicroSound”, ANR-13-LAB1-0005-01 “Fuco-Chem”) and EU project NanoAthero FP7-NMP-2012-LARGE-6-309820.

## References

- [1] S. Yokoyama, H. Ikeda, N. Haramaki, H. Yasukawa, T. Murohara, T. Imaizumi, *J. Am. Coll. Cardiol.* **2005**, 45, 1280; K. Hannawa, B. S. Cho, I. Sinha, K. J. Roelofs, D. D. Myers, T. J. Wakefield, J. C. Stanley, P. K. Henke, G. R. Upchurch, Jr.,

*Ann. N. Y. Acad. Sci.* **2006**, 1085, 353.

- [2] P. A. Barber, T. Foniok, D. Kirk, A. M. Buchan, S. Laurent, S. Boutry, R. N. Muller, L. Hoyte, B. Tomanek, U. I. Tuor, *Ann. Neurol.* **2004**, 56, 116; F. S. Villanueva, E. Lu, S. Bowry, S. Kilic, E. Tom, J. Wang, J. Gretton, J. J. Pacella, W. R. Wagner, *Circulation* **2007**, 115, 345; M. A. McAteer, J. E. Schneider, Z. A. Ali, N. Warrick, C. A. Bursill, C. von zur Muhlen, D. R. Greaves, S. Neubauer, K. M. Channon, R. P. Choudhury, *Arterioscler. Thromb. Vasc. Biol.* **2008**, 28, 77; B. A. Kaufmann, C. Lewis, A. Xie, A. Mirza-Mohd, J. R. Lindner, *Eur. Heart J.* **2007**, 28, 2011; R. Haverslag, G. Pasterkamp, I. E. Hoefer, *Cardiovasc. Hematol. Disord. Drug Targets* **2008**, 8, 252.
- [3] P. Charoenphol, S. Mocherla, D. Bouis, K. Namdee, D. J. Pinsky, O. Eniola-Adefeso, *Atherosclerosis* **2011**, 217, 364.
- [4] P. Saboural, F. Chaubet, F. Rouzet, F. Al-Shoukr, R. B. Azzouna, N. Bouchemal, L. Picton, L. Louedec, M. Maire, L. Rolland, G. Potier, D. L. Guludec, D. Letourneur, C. Chauvierre, *Mar. Drugs* **2014**, 12, 4851.
- [5] F. Rouzet, L. Bachelet-Violette, J. M. Alsac, M. Suzuki, A. Meulemans, L. Louedec, A. Petiet, M. Jandrot-Perrus, F. Chaubet, J. B. Michel, D. Le Guludec, D. Letourneur, *J. Nucl. Med.* **2011**, 52, 1433.
- [6] T. Bonnard, J. M. Serfaty, C. Journe, B. Ho Tin Noe, D. Arnaud, L. Louedec, S. M. Derkaoui, D. Letourneur, C. Chauvierre, C. Le Visage, *Acta Biomater.* **2014**, 10, 3535; L. Bachelet-Violette, A. K. A. Silva, M. Maire, A. Michel, O. Brinza, P. Ou, V. Ollivier, A. Nicoletti, C. Wilhelm, D. Letourneur, C. Menager, F. Chaubet, *RSC Adv.* **2014**, 4, 4864; M. Suzuki, L. Bachelet-Violette, F. Rouzet, A. Beilvert, G. Autret, M. Maire, C. Menager, L. Louedec, C. Choqueux, P. Saboural, O. Haddad, C. Chauvierre, F. Chaubet, J. B. Michel, J. M. Serfaty, D. Letourneur, *Nanomedicine* **2015**, 10, 73.
- [7] P. Couvreur, B. Kante, M. Roland, P. Guiot, P. Bauduin, P. Speiser, *J. Pharm. Pharmacol.* **1979**, 31, 331.
- [8] I. Bertholon, S. Lesieur, D. Labarre, M. Besnard, C. Vauthier, *Macromolecules* **2006**, 39, 3559.
- [9] C. Chauvierre, D. Labarre, P. Couvreur, C. Vauthier, *Macromolecules* **2003**, 36, 6018.
- [10] C. Chauvierre, D. Labarre, P. Couvreur, C. Vauthier, *Pharm. Res.* **2003**, 20, 1786.
- [11] K. Langer, E. Seegmüller, A. Zimmer, J. Kreuter, *Int. J. Pharm.* **1994**, 110, 21.
- [12] C. Chauvierre, L. Leclerc, D. Labarre, M. Appel, M. C. Marden, P. Couvreur, C. Vauthier, *Int. J. Pharm.* **2007**, 338, 327.
- [13] G. Lambert, E. Fattal, H. Pinto-Alphandary, A. Gulik, P. Couvreur, *Pharm. Res.* **2000**, 17, 707.
- [14] G. Yordanov, *Bulg. J. Chem.* **2012**, 1, 61.
- [15] M. Bagad, Z. A. Khan, *Int. J. Nanomedicine* **2015**, 10, 3921.
- [16] C. Vauthier, C. Dubernet, C. Chauvierre, I. Brigger, P. Couvreur, *J. Control. Release* **2003**, 93, 151.
- [17] K. O. Kisich, S. Gelperina, M. P. Higgins, S. Wilson, E. Shipulo, E. Oganessian, L. Heifets, *Int. J. Pharm.* **2007**, 345, 154; C. E. Soma, C. Dubernet, D. Bentolila, S. Benita, P. Couvreur, *Biomaterials* **2000**, 21, 1.
- [18] C. Chauvierre, M. C. Marden, C. Vauthier, D. Labarre, P. Couvreur, L. Leclerc, *Biomaterials* **2004**, 25, 3081.
- [19] M. Liang, N. M. Davies, I. Toth, *Int. J. Pharm.* **2008**, 362, 141.
- [20] G. Lambert, *J. Dispersion Sci. Technol.* **2003**, 24, 439.
- [21] G. Yordanov, C. Dushkin, *Colloid and Polym. Sci.* **2010**, 288, 1019; G. Yordanov, R. Skrobanska, A. Evangelatov, *Colloids Surf. B. Biointerfaces* **2012**, 92, 98; G. Yordanov, A. Evangelatov, R. Skrobanska, *Colloids Surf. B. Biointerfaces* **2013**, 107, 115; G. Yordanov, R. Skrobanska, A. Evangelatov, *Colloids Surf. B. Biointerfaces* **2013**, 101, 215; A. Evangelatov, R. Skrobanska, N. Mladenov, M. Petkova, G. Yordanov, R. Pankov, *Drug Deliv.* **2015**, 14, 1.
- [22] S. Li, Y. He, C. Li, X. Liu, *Colloid Polym. Sci.* **2005**, 283, 480.
- [23] M. C. B. Lira, N. S. Santos-Magalhães, V. Nicolas, V. Marsaud, M. P. C. Silva, G. Ponchel, C. Vauthier, *Eur. J. Pharm. Biopharm.* **2011**, 79, 162.
- [24] C. Vauthier, C. Dubernet, E. Fattal, H. Pinto-Alphandary, P. Couvreur, *Adv. Drug Deliv. Rev.* **2003**, 55, 519.
- [25] Y. Jiao, J. Guo, S. Shen, B. Chang, Y. Zhang, X. Jiang, W. Yang, *J. Mater. Chem.* **2012**, 22, 17636.
- [26] J. M. Chan, L. Zhang, R. Tong, D. Ghosh, W. Gao, G. Liao, K. P. Yuet, D. Gray, J.-W. Rhee, J. Cheng, G. Golomb, P. Libby, R. Langer, O. C. Farokhzad, *Proc. Natl. Acad. Sci.* **2010**, 107, 2213.
- [27] P. Charoenphol, R. B. Huang, O. Eniola-Adefeso, *Biomaterials* **2010**, 31, 1392.
- [28] T. Bonnard, G. Yang, A. Petiet, V. Ollivier, O. Haddad, D. Arnaud, L. Louedec, L. Bachelet-Violette, S. M. Derkaoui, D.

Letourneur, C. Chauvierre, C. Le Visage, *Theranostics* **2014**, 4, 592.

[29] H. Thorlacius, B. Vollmar, U. T. Seyfert, D. Vestweber, M. D. Menger, *Eur. J. Clin. Invest.* **2000**, 30, 804.

[30] C. Foxall, S. R. Watson, D. Dowbenko, C. Fennie, L. A. Lasky, M. Kiso, A. Hasegawa, D. Asa, B. K. Brandley, *J. Cell Biol.* **1992**, 117, 895; A. K. Silva, D. Letourneur, C. Chauvierre, *Theranostics* **2014**, 4, 579.

[31] A. Klink, F. Hyafil, J. Rudd, P. Faries, V. Fuster, Z. Mallat, O. Meilhac, W. J. Mulder, J. B. Michel, F. Ramirez, G. Storm, R. Thompson, I. C. Turnbull, J. Egidio, J. L. Martin-Ventura, C. Zaragoza, D. Letourneur, Z. A. Fayad, *Nat. Rev. Cardiol.* **2011**, 8, 338.

[32] E. Pisani, N. Tsapis, J. Paris, V. Nicolas, L. Cattel, E. Fattal, *Langmuir* **2006**, 22, 4397.

[33] L. Gustafsson, *Talanta*. **1960**, 4, 227.

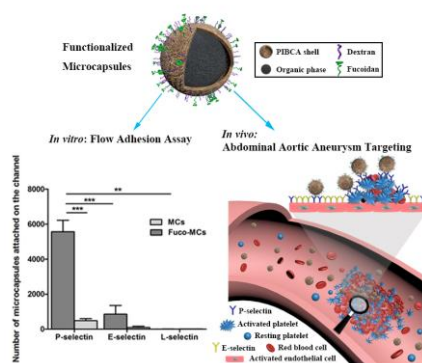
[34] S. Delbosc, J. M. Alsac, C. Journe, L. Louedec, Y. Castier, M. Bonnaure-Mallet, R. Ruimy, P. Rossignol, P. Bouchard, J. B. Michel, O. Meilhac, *PLoS One* **2011**, 6, e18679.

**Table of contents:** Targeted core-shell polymer microcapsules were developed as potential theranostic microcarriers for thrombosis diseases. The microcapsule surface is functionalized by fucoidan, which gives microcapsules the property of specificity to P-selectin under blood flow conditions. Meanwhile, organic core is considered to a potential loading space of probe and/or hydrophobic drug for the diagnosis and/or the treatment of vascular diseases overexpressing P-selectin.

**Keywords:** microcapsules, fucoidan, P-selectin, thrombosis, targeting

**Authors:** Bo Li, Maya Juenet<sup>#</sup>, Rachida Aid-Launais<sup>#</sup>, Murielle Maire, Véronique Ollivier, Didier Letourneur and Cédric Chauvierre

**Title:** Development of fucoidan functionalized polymer microcapsules to target P-selectin overexpressed in cardiovascular diseases



ToC figure.